PHYSICAL REVIEW B VOLUME 37, NUMBER 17 15 JUNE 1988-I

Resonant electron surface-barrier scattering on W(001)

M. N. Read and A. S. Christopoulos
School of Physics, University of New South Wales, P. O. Box 1, Kensington, Sydney, New South Wales 2033, Australia

(Received 8 January 1988; revised manuscript received 17 March 1988)

We have examined very-low-energy electron reflectivity data for W(001) at an angle of incidence of 15° in the [10] azimuth. The structure of the surface barrier is modeled by a one-dimensional saturated image potential, and the metal substrate is modeled by a muffin-tin potential. We have found that below 10 eV, fine-structure surface-barrier scattering features are due to a resonance mechanism where up to seven internal scattering events occur between surface barrier and metal substrate. Previous detailed examinations of fine-structure features have led to the identification of only the interference mechanism in which the features are due to a single scattering between barrier and substrate. When the resonance mechanism occurs, electrons enter above-vacuum quasistable energy states of the surface-barrier potential. The confirmation of the resonance mechanism will allow a parametrized nearly-free-electron scheme to be used to analyze the experimentally obtained features and hence, possibly, to determine the lateral variation of the surface potential on W(001).

In the elastic scattering of low-energy electrons from metal surfaces, a process occurs in which backscattered electrons are scattered between the surface-barrier potential and the metal substrate. This happens when backscattered electrons emerge from the metal substrate with insufficient energy in a direction normal to the surface to surmount the potential barrier and are internally reflected by it. Some electrons may then be backscattered by the metal substrate in such a way that they again cannot escape to the vacuum and are internally reflected. Others may be scattered such that they can escape to the vacuum. The scattering between the barrier and metal substrate can repeat itself a number of times until all electron flux is removed to the vacuum. Under these circumstances electrons are temporarily trapped between substrate and barrier and may be said to occupy an above-vacuum quasistable energy state of the electron surface barrier. This phenomenon has been discussed in detail by McRae.[1] In this work we wish to determine whether this resonant multiple scattering does actually occur on W(001) or whether the number of reflections at the surface barrier is just one.

For the metal and barrier potential models used here, a region of constant potential exists above the metal substrate and the vacuum is also of constant potential. Within these regions the wave function is a sum of plane waves, each of which can be labeled by a wave vector. A beam with a wave vector with a plus superscript indicates that the beam is directed into the metal while a minus superscript indicates that the beam is backscattered from the metal. The incident beam labeled 0 has wave vector $\mathbf{K}_0^+$ in the vacuum and $\mathbf{k}_0^+$ in the region of constant potential above the metal substrate. The amplitude of the specularly backscattered plane wave with wave vector $\mathbf{K}_0^-$ in the vacuum is $b_0(\mathbf{K}_0^-)$ and is given by[1]

$$\underline{b}_0=[\underline{S}^{\mathrm{III}}+\underline{S}^{\mathrm{IV}}\underline{M}(\underline{1}-\underline{S}^{\mathrm{II}}\underline{M})^{-1}\underline{S}^{\mathrm{I}}]\underline{a}_0 . \tag{1}$$

This equation applies for the general case of any number of backscattered beams. The explanation of the symbols is given here for the case of two electron beams with wave vectors $\mathbf{k}_0^-$ and $\mathbf{k}_v^-$, backscattered from the metal substrate. Let the beam v with wave vector $\mathbf{k}_v^-$ have insufficient energy normal to the surface to propagate in the vacuum region (i.e., a preemergent beam). For the case of a one-dimensional surface-barrier model used here, only specular scattering takes place at the barrier and the matrix elements are

$$\underline{b}_0=\begin{pmatrix} b_0(\mathbf{K}_0^-) \\ 0 \end{pmatrix} , \tag{2a}$$

$$\underline{a}_0=\begin{pmatrix} a_0(\mathbf{K}_0^+) \\ 0 \end{pmatrix} , \tag{2b}$$

$$\underline{M}=\begin{pmatrix} \rho_M(\mathbf{k}_0^-\mathbf{k}_0^+) & \rho_M(\mathbf{k}_0^-\mathbf{k}_v^+) \\ \rho_M(\mathbf{k}_v^-\mathbf{k}_0^+) & \rho_M(\mathbf{k}_v^-\mathbf{k}_v^+) \end{pmatrix} , \tag{2c}$$

$$\underline{S}^{\mathrm{I}}=\begin{pmatrix} \tau_b(\mathbf{K}_0^-\mathbf{k}_0^-) & 0 \\ 0 & 0 \end{pmatrix} , \tag{2d}$$

$$\underline{S}^{\mathrm{II}}=\begin{pmatrix} \rho_b(\mathbf{k}_0^+\mathbf{k}_0^-) & 0 \\ 0 & \rho_b(\mathbf{k}_v^+\mathbf{k}_v^-) \end{pmatrix} , \tag{2e}$$

$$\underline{S}^{\mathrm{III}}=\begin{pmatrix} \rho_b(\mathbf{K}_0^-\mathbf{K}_0^+) & 0 \\ 0 & 0 \end{pmatrix} , \tag{2f}$$

$$\underline{S}^{\mathrm{IV}}=\begin{pmatrix} \tau_b(\mathbf{k}_0^+\mathbf{K}_0^+) & 0 \\ 0 & 0 \end{pmatrix} . \tag{2g}$$

The amplitude of the incident plane wave with wave vector $\mathbf{K}_0^+$ is given by $a_0(\mathbf{K}_0^+)$. Elements like $\rho(\mathbf{k}_x^{\mp}\mathbf{k}_y^{\pm})$ with $x=0$ or v and $y=0$ or v represent an amplitude reflection coefficient for a plane wave with wave vector $\mathbf{k}_y^{\pm}$ being scattered to a plane wave with wave vector $\mathbf{k}_x^{\mp}$. Elements like $\tau(\mathbf{K}_x^{\pm}\mathbf{k}_y^{\pm})$ represent an amplitude transmission coefficient for a plane wave with wave vector

$\mathbf{k}_y^{\pm}$ being scattered to a plane wave with wave vector $\mathbf{K}_x^{\pm}$. The subscript b refers to the surface barrier while M refers to the metal substrate potential.

It can be proven that in the present instance for the general case of any number of beams, the matrix inversion $(\underline{1}-\underline{S}^{II}\underline{M})^{-1}$ can be expanded as

$$\underline{1}+\underline{S}^{II}\underline{M}+(\underline{S}^{II}\underline{M})^2+(\underline{S}^{II}\underline{M})^3+\cdots . \tag{3}$$

Therefore on expanding out the matrices in Eq. (1) we obtain

$$\underline{b}_0=[\underline{S}^{III}+\underline{S}^{IV}\underline{M}\underline{S}^{I}+\underline{S}^{IV}\underline{M}\underline{S}^{II}\underline{M}\underline{S}^{I}+\underline{S}^{IV}\underline{M}(\underline{S}^{II}\underline{M})^2\underline{S}^{I}+\underline{S}^{IV}\underline{M}(\underline{S}^{II}\underline{M})^3\underline{S}^{I}+\cdots]\underline{a}_0 . \tag{4}$$

For energies greater than a few eV above the vacuum $\rho_b(\mathbf{k}_0^+\mathbf{k}_0^-)$ and $\rho_b(\mathbf{K}_0^-\mathbf{K}_0^+)$, representing internal and external reflection of the incident beam at the surface barrier, respectively, are negligible. For illustrative purposes here these quantities are set to zero in the following explanation although they are included in the actual computations. Equation (4) then becomes explicitly, in the case of two backscattered beams,

$$\begin{aligned} b_0(\mathbf{K}_0^-)=\{&\tau_b(\mathbf{k}_0^+\mathbf{K}_0^+)\rho_M(\mathbf{k}_0^-\mathbf{k}_0^+)\tau_b(\mathbf{K}_0^-\mathbf{k}_0^-)+\tau_b(\mathbf{k}_0^+\mathbf{K}_0^+)\rho_M(\mathbf{k}_v^-\mathbf{k}_0^+)\rho_b(\mathbf{k}_v^+\mathbf{k}_v^-)\rho_M(\mathbf{k}_0^-\mathbf{k}_v^+)\tau_b(\mathbf{K}_0^-\mathbf{k}_0^-)\\ &+\tau_b(\mathbf{k}_0^+\mathbf{K}_0^+)\rho_M(\mathbf{k}_v^-\mathbf{k}_0^+)\rho_b(\mathbf{k}_v^+\mathbf{k}_v^-)\rho_M(\mathbf{k}_v^-\mathbf{k}_v^+)\rho_b(\mathbf{k}_v^+\mathbf{k}_v^-)\rho_M(\mathbf{k}_0^-\mathbf{k}_v^+)\tau_b(\mathbf{K}_0^-\mathbf{k}_0^-)\\ &+\tau_b(\mathbf{k}_0^+\mathbf{K}_0^+)\rho_M(\mathbf{k}_v^-\mathbf{k}_0^+)\rho_b(\mathbf{k}_v^+\mathbf{k}_v^-)\rho_M(\mathbf{k}_v^-\mathbf{k}_v^+)\rho_b(\mathbf{k}_v^+\mathbf{k}_v^-)\rho_M(\mathbf{k}_0^-\mathbf{k}_v^+)\tau_b(\mathbf{K}_0^-\mathbf{k}_0^-)\\ &+\tau_b(\mathbf{k}_0^+\mathbf{K}_0^+)\rho_M(\mathbf{k}_v^-\mathbf{k}_0^+)[\rho_b(\mathbf{k}_v^+\mathbf{k}_v^-)\rho_M(\mathbf{k}_v^-\mathbf{k}_v^+)]^3\rho_b(\mathbf{k}_v^+\mathbf{k}_v^-)\rho_M(\mathbf{k}_0^-\mathbf{k}_v^+)\tau_b(\mathbf{K}_0^-\mathbf{k}_0^-)+\cdots\}a_0(\mathbf{K}_0^+) . \end{aligned} \tag{5}$$

The scattering processes represented by each term in Eq. (5) are shown in Fig. 1 and described in the caption. The phase difference between the direct and indirect contributions to the amplitude of backscattered beam 0 gives rise to a fluctuation in the reflectivity profile which we call a barrier scattering feature. In the case where a multiple scattering between substrate and barrier occurs we have a *resonance* mechanism where the electron temporarily enters an above-vacuum energy state of the surface barrier. In the case of only one internal scattering at the surface barrier, we simply have an *interference* mechanism which is not associated with energy states of the surface barrier.

In the analysis of fine-structure barrier scattering features in the electron reflectivity data of Cu(001) for incident angles of $\theta=67.5°$ and $\phi=45°$, Dietz, McRae, and Campbell[2] found that they needed to include only a single internal scattering of preemergent beams at the surface barrier in the calculation of the backscattered probability. Following this work, Le Bossé *et al.*[3] examined these low-energy beam threshold effects on Ni(001) for $\theta=58°$ and $\phi=45°$, on Al(001) for $\theta=0°$, and on W(001) for $\theta=48°$ and $\phi=45°$; and Gaubert *et al.*[4] reexamined Cu(001) for $\theta=61.7°$ and $\phi=45°$. These studies reported that the mechanism involved in all these cases was due to the interference effect and cast doubt on whether the resonance mechanism actually occurred in any real case.

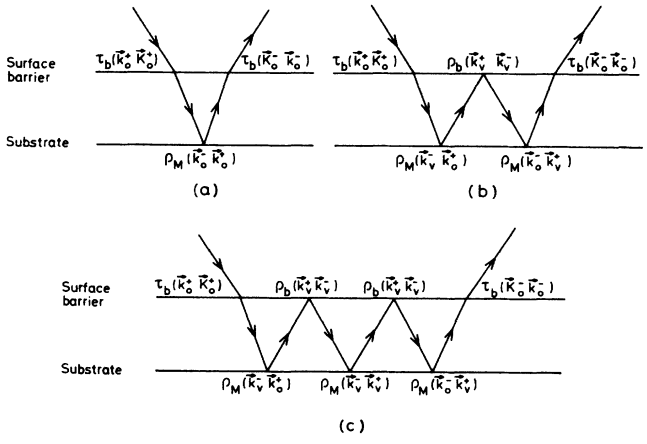

FIG. 1. Direct and indirect scattering events occurring between a one-dimensional surface potential barrier and the two-dimensional metal substrate potential for the case of one emergent beam labeled 0 and one preemergent beam labeled v. (a) represents direct scattering of beam 0, (b) represents first-order indirect scattering involving beam v, while (c) shows second-order indirect scattering where two internal scatterings at the surface barrier occur involving beam v.

A systematic study of polarized electron scattering from W(001) at angles θ from 15° to 37.5° in 2.5° steps by Pierce and co-workers[5,6] showed a splitting of spin-up and spin-down reflectivity peaks at very low energies, <10 eV. For incident angles less than 26° the peak splitting was found to be proportional to peak width, and this result is consistent with McRae's scattering theory[1] with only a single internal scattering event at the surface potential barrier (i.e., the interference regime). For angles less than 26° the above proportionality was not observed, and this is consistent with multiple scattering occurring between substrate and barrier (i.e., the resonance regime).

A computation of spin-dependent reflectivities for these scattering conditions has been performed by Jennings and Jones[7] and Jones and Jennings.[8] In these calculations only indirect scattering to first order was included (i.e., a single internal scattering event between barrier and substrate) and good qualitative agreement with experimental data was found for the larger incident angles $\theta=48°$ and 43°. For $\theta=26°$ and 15°, although there is some qualitative agreement between calculation and experiment for some features, other prominent features do not correlate. It is then still possible that higher-order scattering events may make a contribution to the profiles for $\theta<26°$ and that this may have been previously overlooked.

Experimental intensity data for the 00 beam on

W(001) at $\theta=16°$ has been collected by McRae and Wheatley[9] for 0–10 eV, showing two peaks at about 4 and 6 eV each. The 4-eV feature is believed to be associated with a Bragg peak arising from a gap in the spin-dependent bulk band structure,[6] which would only be produced from a spin-dependent scattering treatment. However, the spin-free and spin-dependent calculations of Jones and Jennings[8] show very little difference for $\theta=15°$. The details of the spectra also strongly depend on the contraction of the surface layer on W(001) as well as the details of the surface-barrier model and the substrate scattering potential.[10] For these reasons no attempt is made to exactly fit the experimental data in these initial calculations, and spin-up and spin-down reflectivities will not be computed separately, rather the average backscattered reflectivities of spin-up and spin-down electrons will be computed. A zero contraction of the surface layer will also be used. The aim is to determine whether or not a resonance scattering mechanism may possibly exist on W(001) for $\theta<26°$ at very low energies, rather than to exactly fit the experimental data.

The muffin-tin scattering potential used for W is that due to Mattheis,[11] and atomic scattering is treated relativistically. Interatomic scattering, however, is treated nonrelativistically with the spin-up and spin-down phase shifts averaged. The average elastic scattering potential between muffin-tin spheres U_{el} is taken as the zero of energy. The inelastic scattering potential in the bulk crystal U_{in}, in the energy range 0.6–10 eV, is taken as

$$-U_{in}(E)=0.5E^{1/3}\,\text{eV}\ , \tag{6}$$

where E is the energy of the incident electrons with respect to the vacuum level. The electron scattering potential of the surface conduction electrons is the surface-barrier potential U^b. Its elastic part U^b_{el} is modeled by the average one-dimensional linear saturated image barrier (SIB) first suggested in Ref. 2 and described in detail in Ref. 12. The parameters of the surface-barrier model used for W(001) are $U_0=15$ eV, $U_s=0$ eV, and $z_0=-6.0$ a.u. (−3.2 Å) and $z_j=-1.7$ a.u. (−0.9 Å). U_0 is the height of the potential-energy barrier, and U_s is the value of the potential-energy barrier with respect to the crystal zero of potential at the point z_j. z_j is the join point of the constant potential between the muffin-tin spheres and the surface potential barrier. z_0 is the origin of the image potential form. The z coordinate axis points into the crystal and is perpendicular to the first row of atoms at the surface with origin at the center of this layer. Two different models of surface inelastic scattering potential U^b_{in} were employed, as the inelastic scattering in the surface-barrier region is likely to have a significant effect on whether single or multiple reflections between barrier and metal substrate occur. In one model, the constant bulk inelastic potential U_{in} which extends up to $z=0$ is extended into the vacuum as a half-Gaussian function with half-width $a\cong 1$ Å and with no lateral variation along the surface. Details of the half-Gaussian function are described in Ref. 12. As this model may overestimate inelastic scattering, another model which included no surface inelastic scattering was also used for comparison.

Figure 2 shows our calculations of the surface-barrier

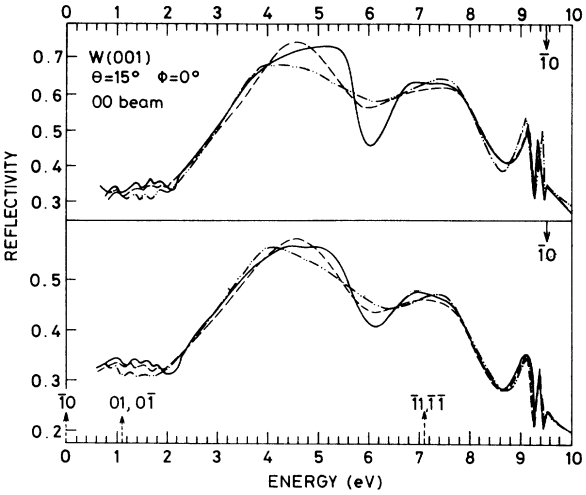

FIG. 2. Reflectivity of the 00 beam of electrons elastically scattered at an incident polar angle of 15° along the [10] azimuth, from the W(001) surface. Downward arrows indicate the energies of emergence of beams in the vacuum, while upward arrows indicate energies of emergence of beams from the metal substrate. The full curve shows results for the exact calculation including all orders of multiple scattering between metal substrate and surface barrier; the dot-dashed curves are results obtained by including one internal scattering event between substrate and barrier; the dashed curves are results from including two internal substrate-barrier scattering events. Curves in the upper frame include no inelastic scattering in the surface region; curves in the lower frame include inelastic scattering in the surface region by extending the bulk inelastic scattering potential with a half-Gaussian function centered at the origin as described in the text.

scattering features produced in the 00 beam average-reflectivity profile of spin-up and spin-down electrons for W(001) at $\theta=15°$ in the [01] azimuth using the Kambe-McRae method.[13] The upper frame shows results with the exclusion of any inelastic scattering in the surface-barrier region, while the lower frame includes surface inelastic scattering as described in the preceding paragraph. The computations were performed with an energy interval of 0.1 eV. The full curves show the results of the exact calculation using Eq. (1) with the inclusion of 13 beams. The dot-dashed curves show the reflectivity using Eq. (4) with 13 beams and retaining the first three terms (i.e., indirect scattering to first order) while the dashed curves are the same result retaining the first four terms (i.e., indirect scattering to second order). In this energy range, three sets of nonspecular beams have emerged from the substrate but not yet into the vacuum, and these beams give rise to the Rydberg series of barrier scattering features. The $\bar{1}0$ beam is emerged from the metal substrate for the energy of 0 eV in the vacuum; the $01,0\bar{1}$ set emerges at 1.13 eV and the $\bar{1}1,\bar{1}\bar{1}$ set emerges at 7.11 eV. The overall shape of the profile is determined by the fine structure associated with barrier scattering being superimposed on the Bragg peak occurring at ~4.8 eV. The fine structure, in turn, is a mixture of the Rydberg series for each of the three beam sets mentioned above. The weak fine

structure below 2 eV is mainly due to indirect scattering of the backscattered specular beam between substrate and barrier. The structure above 8 eV is due entirely to the $\bar{1}0$ beam. Between 4 and 8 eV the structure is a mixture of Rydberg series for the $\bar{1}0$ and $01,0\bar{1}$ beam sets. It is found that the $\bar{1}1,\bar{1}\,\bar{1}$ set has no effect on the profile in the energy range considered. In the lower frame, peak and trough locations differ by up to 0.8 eV between the exact and first-order indirect scattering cases, while differences up to 0.2 eV exist between exact and second-order indirect scattering features. When no surface inelastic scattering is included, as in the top frame, the differences are even larger. It was necessary to include indirect scattering, as illustrated in Fig. 1, to seventh order to obtain agreement with the exact result to three significant figures over the total-energy range for the profile in the lower frame. This shows that, with the surface inelastic scattering potential used, up to seven scattering events between barrier and substrate occur. For the top frame which includes no inelastic surface scattering, up to 20th-order indirect scattering must be used to obtain the same result as the exact case.

The fact, that Jones and Jennings[8] found the contribution to the reflectivity from second and higher orders of indirect scattering on W(001) was negligible, is, we believe, due to the fact that they appear to aim only to reproduce experimental features to within about 2 eV in their theoretical calculations for low incident angles. When attempting to determine the form of the surface barrier with this level of discrepancy between theory and experiment, the changes due to higher-order indirect scattering may indeed by negligible. However, it has been shown[12] that, at least for large incident angles, matches to at least 0.05 eV are necessary in order to determine the surface-barrier shape and parameters. From this work it is seen that higher-order indirect scattering terms should be included in any surface-barrier structure determination for W(001) using low-angle data.

This is the first time that a resonance or multiple scattering mechanism has been identified directly from a realistic calculation. In this case, an electron with a certain parallel component of wave vector is temporarily trapped in an above-vacuum surface-barrier energy state, or surface-barrier resonance state. Further studies on W(001) at other angles is now in progress to determine the extent of the resonance processes. It appears that a wealth of resonance features is present in reflectivity data on W(001) at low energies and angles, which means that experimental data can be analyzed very simply to determine the surface-state dispersion. If the dispersion is nearly-free-electron-like, the parametric theory of McRae, Landwehr, and Caldwell[14] could be used to determine the binding energies of the states, the laterally average surface potential, and hence the lateral atomic positions at the surface. This is a potentially powerful technique for surface-structure analysis.

[1]E. G. McRae, Rev. Mod. Phys. **51**, 541 (1979).
[2]R. E. Dietz, E. G. McRae, and R. L. Campbell, Phys. Rev. Lett. **45**, 1280 (1980).
[3]J. C. Le Bossé, J. Lopez, G. Gaubert, Y. Gauthier, and R. Baudoing, J. Phys. C **15**, 3425 (1982); **15**, 6087 (1982).
[4]G. Gaubert, R. Baudoing, Y. Gauthier, J. C. Le Bossé, and J. Lopez, J. Phys. C **16**, 2625 (1983).
[5]D. T. Pierce, R. J. Celotta, G.-C. Wang, and E. G. McRae, Solid State Commun. **39**, 1053 (1981).
[6]E. G. McRae, D. T. Pierce, G.-C. Wang, and R. J. Celotta, Phys. Rev. B **24**, 4230 (1981).
[7]P. J. Jennings and R. O. Jones, Solid State Commun. **44**, 17 (1982).
[8]R. O. Jones and P. J. Jennings, Phys. Rev. B **27**, 4702 (1983).
[9]E. G. McRae and G. H. Wheatley, Surf. Sci. **29**, 3442 (1972).
[10]H.-J. Herlt, R. Feder, G. Meister, and E. G. Bauer, Solid State Commun. **38**, 973 (1981).
[11]L. F. Mattheiss, Phys. Rev. **139**, 236 (1965).
[12]M. N. Read, Phys. Rev. B **32**, 2677 (1985).
[13]K. Kambe, Z. Naturforsch. Teil A **22**, 322 (1967); **23**, 1280 (1968); E. G. McRae, Surf. Sci. **11**, 479 (1968); **25**, 491 (1971).
[14]E. G. McRae, J. M. Landwehr, and C. W. Caldwell, Phys. Rev. Lett. **38**, 1422 (1977).